

Wear monitoring of journal bearings with acoustic emission under different operating conditions

José-Luis Bote-Garcia, Noushin Mokhtari, and Clemens Gühmann

Chair of Electronic Measurement and Diagnostics Technology, Technische Universität Berlin, Berlin, Germany

jose-luis.bote-garcia@tu-berlin.de

noushin.mokhtari@tu-berlin.de

clemens.guehmann@tu-berlin.de

ABSTRACT

It has been shown that Acoustic Emission (AE) can be used to classify different friction states and identify defects in journal bearings. In addition, it has been demonstrated in experimental setups that AE can be used to estimate the wear volume of sliding lubricated metallic contacts. The aim of our work is to monitor the wear during the operation of a journal bearing. This work deals with the development of a prognosis system for a detection of the wear and its volume by means of AE before an actual fault occurs. For this purpose, a journal bearing test bench was developed, where the oil temperature for the lubrication, load and rotational speed can be set. Experiments were carried out under different operating conditions and lasted up to 20 hours each. To establish a correlation between wear and AE, the wear volume is determined by comparing recorded roundness profiles of the inner race before and after each experiment at multiple positions. The method used is validated by measuring the roughness of the inner race surface, thus confirming the position of the wear. The analysis of the recorded AE signals shows an amplitude modulation as well as bursts. The frequency of the amplitude modulation correlates with the rotational speed even at higher velocities. Bursts in the AE signal are directly related to wear. Various features, e.g. root mean square value and properties of the measured bursts, of the AE signal and their relevance for the prediction of the wear are analyzed. A quantitative estimation of the volume proves to be challenging, while a qualitative estimation of occurrence and severity of wear can be reliably detected.

1. INTRODUCTION

The detection of damages and the prediction of wear is the basis of a system for prognostic health management. When monitoring the wear due to sliding friction it is demonstrated

that AE is capable to capture changes caused by frictional force and material removal in experimental setups (Hase, Mishina, & Wada, 2012; Hase, Mishina, & Wada, 2016). The AE is generated by elastic stress waves emitted due to deformation and fracture of material which is caused by friction and progressing wear. Bearings are a crucial element of rotating machinery and are a main cause of breakdowns due to defects. With regard to journal bearings only little work is done to establish a link between the ongoing wear and AE. This is necessary to perform a non-destructive online-wear measurement. The aim of our work is on the prediction of wear rate and thus the Remaining Useful Lifetime (RUL) of a hydrodynamic journal bearing.

AE generates signals with frequencies ranging from 50 kHz to 2 MHz (Albers & Dickerhof, 2010). Two phenomena are of interest for the monitoring of a journal bearing: amplitude modulation and bursts. The frequency of the amplitude modulation correlates with the rotational speed of the shaft and is caused by misalignment of the bearing and the shaft (Chacon et al., 2014). The bursts are produced due to the generation of wear particles (Hase et al., 2012).

Several researchers showed that it is possible to distinguish between the mixed, solid and fluid friction by means of AE (Mokhtari, Knoblich, Nowoisky, Bote-Garcia, & Gühmann, 2019; Albers, Burger, Scovino, & Dickerhof, 2006). In the case of hydrodynamic journal bearings the bearing surface and the journal surface are separated by a lubricant film generated by the journal rotation. At lower rotational speeds this supporting lubricant film is not formed. Therefore it is assumed that the bigger part of wear is produced during this unfavorable mixed and solid friction.

It is shown that with AE it is possible to capture seeded defects (Elasha, Greaves, Mba, & Fang, 2017) and seizures in journal bearing in an early stage (Hase et al., 2016). Here high-frequency components, frequencies higher than 1 MHz, indicate the beginning of a seizure. In two other works it is stated that the amplitude modulation is suitable to detect

José-Luis Bote-Garcia et al. This is an open-access article distributed under the terms of the Creative Commons Attribution 3.0 United States License, which permits unrestricted use, distribution, and reproduction in any medium, provided the original author and source are credited.

continuous rubbing in seals of turbines (Hall & Mba, 2004; Leahy, Mba, Cooper, Montgomery, & Owen, 2006).

In earlier studies on wear, experimental setups had already shown that AE is related to the wear rate and the material removed for lubricated sliding contacts (Boness & McBride, 1991; Hase et al., 2012). Therefore it is evident that such a connection also exists for journal bearings. However no system for the wear prediction exists. One reason for this may be that it proved to be challenging to measure the wear.

Even though AE is more complex to measure than vibration due to the high frequencies, it is more suitable for detecting damage and unfavorable operating conditions (Hall & Mba, 2004; Leahy et al., 2006; Chacon et al., 2014). The lower frequency ranges detected by the vibration signals are usually overlaid by other signals produced from rotating machinery, making it difficult or impossible to distinguish between the signal sources. The AE operating at higher frequencies is not overlaid by other machine parts. With vibration signals it is possible to detect damages in an advanced, meanwhile AE is suitable to detect a damage earlier (Elasha et al., 2017). In (Li & Cheng, 2009) different reasons are discussed why vibration signals are not suitable for monitoring friction in a steam turbine. It can therefore be assumed that AE is better suited to monitor ongoing wear mechanisms than the vibration signal.

This work presents results of our ongoing research on a system for online wear prediction for journal bearings. The aim of this research is to estimate the wear to determine the optimal time for replacement and therefore the RUL. At first the test bench, the measuring systems and methods are presented. Several experiments are carried out. Then the results of the signal analysis are presented. In the end a classifier is trained and validated to detect the occurrence of wear during an experiment.

2. EXPERIMENTS

All experiments were carried out on an temperature-controlled test bench described in (Mokhtari et al., 2019).

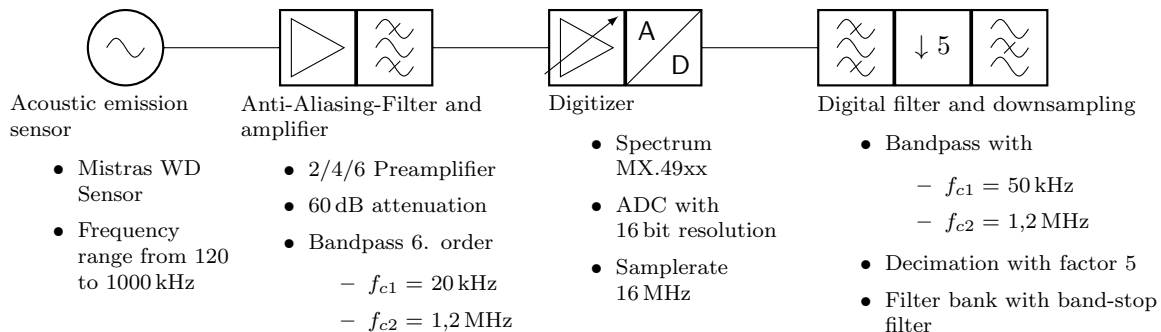


Figure 1. Measurement chain used for the acquired AE signal. A decimation and multiple filters are necessary to reduce the amount of data.

2.1. Test Bench

The setup consists of two rolling bearings that support the shaft which is driven by a servomotor. Between the two supporting bearings the journal bearing is placed. A hydraulic pressure unit is used to apply a load onto the journal bearing. All parts are mounted on a test bed, thus the journal bearing can be installed and removed as easily as possible. For controlling the lubrication temperature and thereby viscosity of the oil, a temperature control system is placed below the setup. The test bench allows to set the mean surface pressure \bar{p} , thus the load, oil inlet temperature $T_{oil,in}$ and oil inlet pressure $p_{oil,in}$, and rotational speed n_{an} . Table 1 gives an overview of the parameters of the test bench used for the experiments.

Table 1. Overview of the conditions of experiments conducted. Rotational speed n_{an} , mean surface pressure \bar{p} and oil inlet temperature $T_{oil,in}$ were changed over the course of the experiments conducted.

Component	Value
Bearing bush diameter D_B	50 mm
Bearing bush width B	25 mm
Rotational speed n_{an}	30 rpm to 400 rpm
Mean surface pressure \bar{p}	5 bar to 80 bar
Bearing bush material	red bronze RG7
Shaft material	ST52-3
Oil	Hydraulic oil CKT 68
Oil inlet temperature $T_{oil,in}$	40 °C to 60 °C
Oil inlet pressure $p_{oil,in}$	1 bar

2.2. Data acquisition

For the acquisition of the AE signals a wideband piezoelectric sensor is used. It has a frequency range ranging from 100 to 900 kHz and is installed together with a temperature sensor on the front side of the bearing support. The measurement chain for the AE sensor is shown in figure 1. Following the AE sensor an amplifier and bandpass filter is used. To digitize the AE signal an ADC with 16 bit resolution is used. The sample frequency is set to 16 MHz. After digitalization the signal is filtered with a bandpass filter as well as several

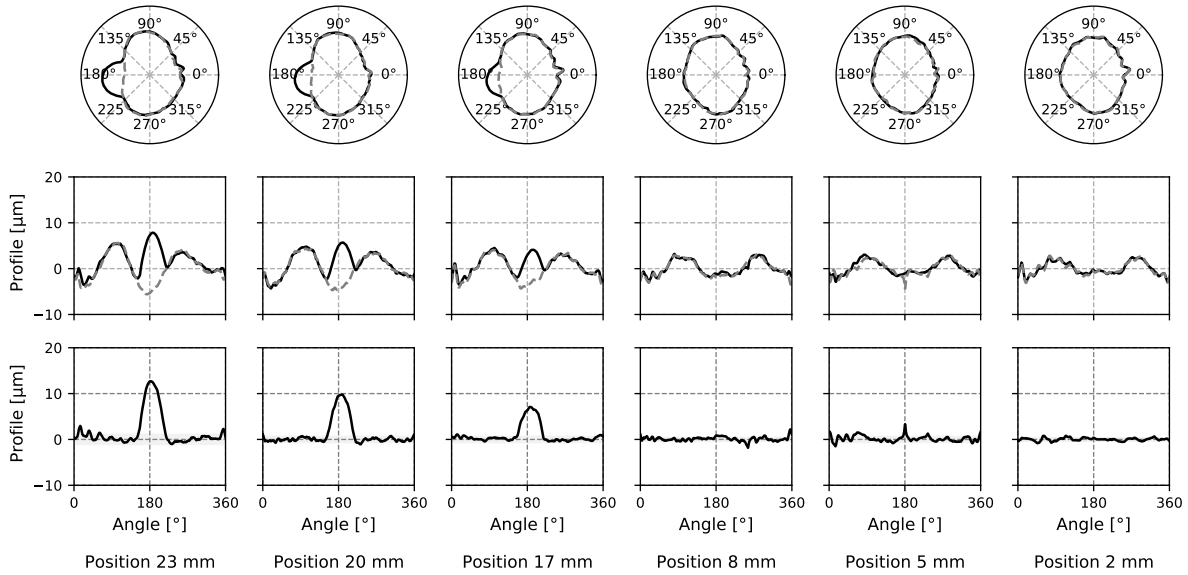


Figure 2. Roundness profile matching. The initial roundness profiles are shown in the upper two lines in grey and dashes. The roundness profiles after the experiment are shown in black. The lower line shows the difference between the initial and following roundness profiles. At the positions 23, 20 and 17 mm the progressing wear is visible.

bandstop filters and down sampled by a factor of five to remove interfering signals and to reduce the amount of data. In the end the signals have a sample rate of 3,2 MHz. All other signals are sampled at a lower frequency at 20 kHz.

2.3. Measuring wear

To observe the wear before and after each experiment the roughness of the inner race and the roundness of the inner face of the journal bearing are measured at certain locations as illustrated in figure 3. The surface roughness is measured along the total length of the inner race every 30° beginning at 30° with an ACCRETECH SURFCOM TOURCH 50. The roundness is acquired at six positions neither too close to the outer edge nor too close the oil inlet with a Zeiss RONDCOM Touch.

The initial roundness profiles for one journal bearing are centered using the least square circle. After one experiment the roundness profiles are measured at the same positions and matched to the initial roundness profiles. This is illustrated in figure 2 for one experiment. Roundness measurements at different locations are shown in the upper two rows. The initial profiles are plotted in grey and dashed. The profiles acquired after the experiment are plotted in black. The lower row shows the difference between the roundness measurements. At the positions of 23 mm, 20 mm and 17 mm the progression of the wear can be seen. Using the difference of the roundness profiles and the positions at which the profiles were acquired the volume of the occurred wear can be estimated.

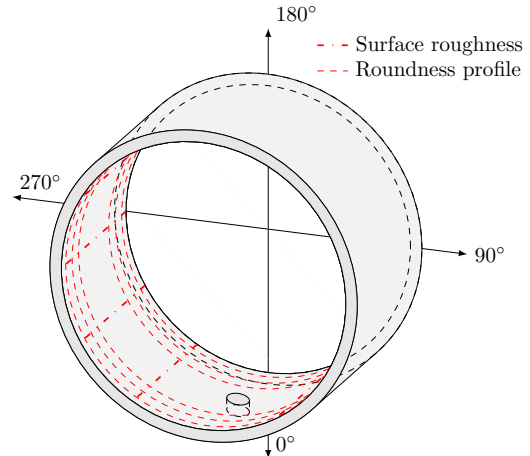


Figure 3. The red lines indicate where the progressing wear is analyzed for each bearing by measuring the surface roughness and the roundness profile.

For the same experiment the location of the wear is confirmed by the change of the surface roughness of the inner race as one can see in figure 4. Here the change of roundness profiles before and after an experiment and the surface roughness are plotted side by side. A qualitative comparison shows that the change in the roundness profile and the surface roughness correlate.

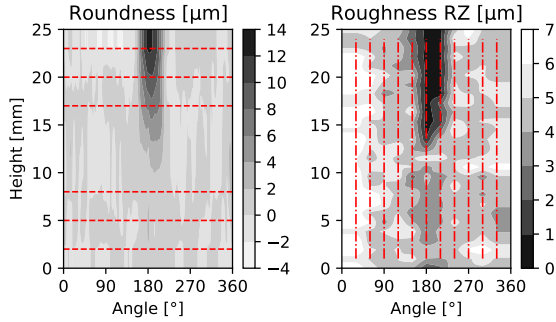


Figure 4. Comparison of roundness profile (left) and surface roughness (right) of the inner race of a bearing. The location of the measurements are highlighted by the dashed lines. The location of the progressing wear in the roundness profiles matches to the surface roughness.

2.4. Experimental Procedure

The condition, surface roughness and roundness of the journal bearing are recorded before and after each experiment. The experiments conducted lasted up to 20 h. Every 5 min all sensor signals,

- acoustic emission AE
- journal bearing temperature
- rotational speed n_{an}
- mean surface pressure \bar{p}

are recorded for 20 s. A continuous recording is not possible due to the sheer amount of data.

2.5. Experiments conducted

In total 22 experiments were conducted and three bearings were used. The total wear depth and maximal wear volume that had occurred are shown in table 2. For a large part of the experiments the rotational speed n_{an} , mean surface pressure \bar{p} and oil inlet temperature $T_{oil,in}$ were set at the beginning and were held constant. With bearing number 0 experiments with varying conditions were conducted, i.e. the applied load was changed during the experiment to increase the wear.

Table 2. Number of experiments conducted and the total wear for each bearing.

Bearing	Experiments conducted	Maximal depth of wear w_d [μm]	Total volume of wear w_V [mm^3]
0	6	12,0	2,8
1	4	23,2	3,6
2	12	54,8	10,6

3. DATA EVALUATION

The analysis of the acquired AE signals shows an amplitude modulation of the envelope as well as bursts.

3.1. Amplitude Modulation

The amplitude modulation depends on the operating point and the condition of the bearing. It can be observed that the characteristics of the amplitude modulation at constant operating conditions, i.e. the load, speed and oil temperature, vary during an experiment. The amplitude modulation can be analyzed by calculating the envelope of the AE signal.

In figure 5 an example of an AE Signal is shown. First a clip from the 20 s long measurement and its envelope is plotted. Below, in the Short-Time Fourier Transformation (STFT) one can see that the main energy of the AE is concentrated around 100 kHz. The lowermost plot shows the Discrete Fourier Transform (DFT) of the envelope. The spectrum of the envelope showed peaks at the positions of the rotational speed and integer multiples indicating the first and higher harmonics. The amplitude of these harmonics changed over time during an experiment.

3.2. Burst

Bursts in the AE signal occurred in most experiments but the amplitude and the quantity varied greatly. An example of a burst with a relatively high amplitude is shown in figure 6. The upper plot shows a burst in the AE signal and its envelope. The STFT of the burst shows that the energy of the burst is distributed over a wide frequency band. The bottom plot shows again the DFT of the envelope and a distinct peak at the location of the first harmonic.

The acquired data indicate that bursts occur even at operational conditions with no measurable wear and under fluid friction. However their amplitude and thereby their energy is much lower and they appear less frequent. Under some conditions the bursts were hardly detectable in the time domain as one can suspect when observing the burst in figure 5 around 0,7 s. In experiments with a lot of measurable wear the occurrence of violent bursts is more frequent meaning that the amplitude and their energy is higher.

3.3. Features

In order to investigate the relationship between wear and AE signals several features were utilized. Those features were acquired for each measurement of the AE signal AE and its envelope E . Table 3 lists all used features.

From AE the Root-Mean Square (RMS) value RMS_{AE} and maximal value max_{AE} is calculated. Starting from E the RMS value RMS_E , mean value $\hat{\mu}_E$ and variance $\hat{\sigma}_E^2$ is determined. Furthermore the number of peaks $\#Burst_{500}$ exceeding 500 mV is counted and the mean value $\mu_{Burst_{500}}$ of their peaks is calculated. In addition a less strict threshold is determined for each measurement AE and used to obtain the number of peaks $\#Burst_T$ and their mean peak value μ_{Burst_T} . The threshold is set to $T = \hat{\mu}_E + 3 \cdot \hat{\sigma}_E^2$. If no

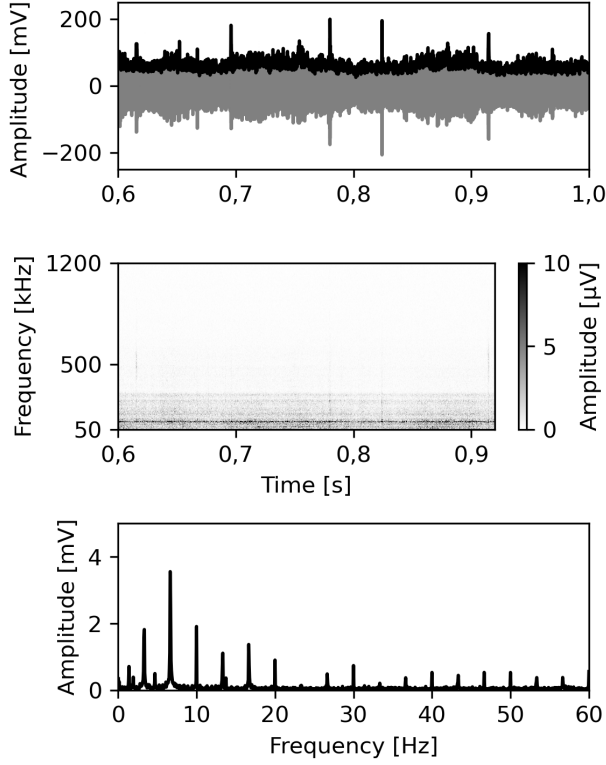


Figure 5. The upper plot shows the AE signal (grey) and its envelope (black). The second plot shows the STFT of the AE signal. The third plot shows the DFT of the envelope with peaks visible at the location of the rotational speed and integer multiples.

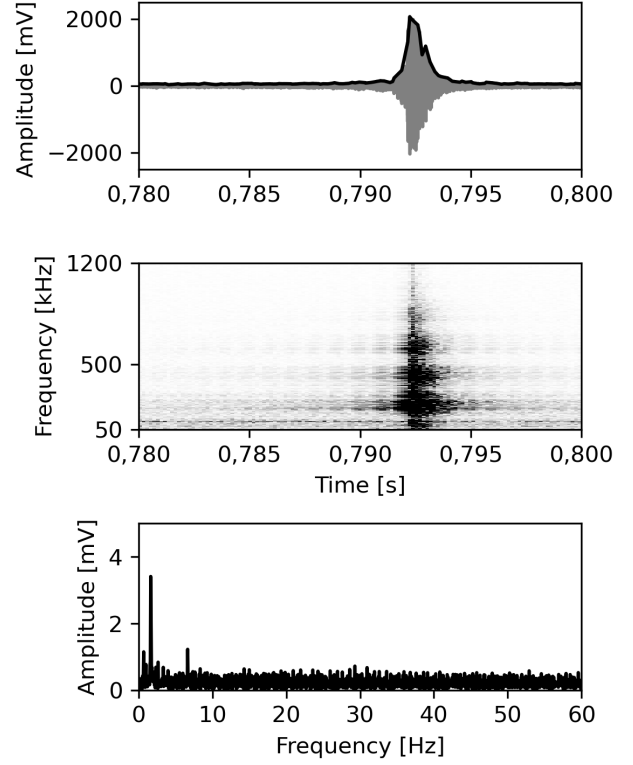


Figure 6. The upper plot shows a single burst in the AE signal (grey) and its envelope (black). The second plot shows the STFT of the AE signal. The third plot shows the DFT of the envelope. The burst is in particular visible in the higher frequencies of the STFT.

Table 3. Overview of the used features.

Feature	Description
RMS_{AE}	$\sqrt{\frac{\sum_{n=1}^N AE[n]^2}{N}}$
max_{AE}	$\max AE$
RMS_E	$\sqrt{\frac{\sum_{n=1}^N E[n]^2}{N}}$
$\#Burst_{500}$	Number of bursts above 500 mV
$\mu_{Burst_{500}}$	$\frac{\sum_{n=1}^{\#Burst_{500}} Burst_{500}[n]}{\#Burst_{500}}$
$\#Burst_T$	Number of bursts above T mV
μ_{Burst_T}	$\frac{\sum_{n=1}^{\#Burst_T} Burst_T[n]}{\#Burst_T}$
f_{H_1}	Frequency of the first harmonic
$\arg(f_{H_1})$	Amplitude of f_{H_1}

burst is found, $\mu_{Burst_{500}}$ and μ_{Burst_T} are set to 0. Finally the frequency of the first harmonic f_{H_1} from the DFT of E and its value $\arg(f_{H_1})$ are obtained.

Figure 7 shows selected features over the course of two experiments. One experiment where wear was measured and the other experiment with no measurable wear. It can be observed that the features in case of wear are less steady and fluctuate. It is also notable that bursts $\#Burst_T$ occur in the case of no measurable wear but their mean amplitude μ_{Burst_T} is smaller.

4. CLASSIFICATION

For classification a Random Forest Classifier (RFC) is used. It is a simple but powerful classifier with good characteristics regarding over-fitting if the number of decision trees is set high enough. The RFC combines a number of decision trees, whereby each one is built from a sample of the training set (Breiman, 2001). In addition a RFC returns a measure of feature importance. This is done by adding up the decrease of impurity for a feature when it is used for a split in a node of a single tree. This is done over all trees and averaged.

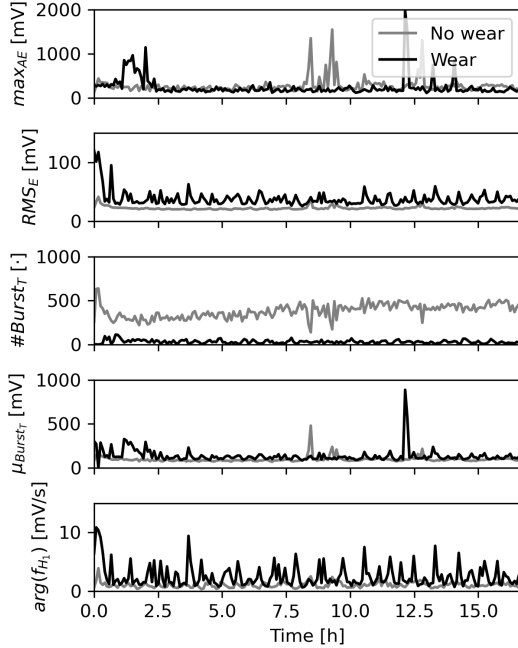


Figure 7. Selected features over the course of two experiments. In the case of 'No wear' bursts $\#Burst_T$ can be detected but the mean amplitude μ_{Burst_T} is lower.

A Leave-One-Out Cross-Validation (LOOCV) is used for validation. As described in section 2.5, experiments were performed with three different bearings. The data from two experiments are used for training a RFC and the left out experiment is used for validation. The features detailed in section 3.3 are calculated for each of the 20s measurement of an experiment. Finally, the mean value of all features for an experiment is calculated. The measured wear w_V of each experiment is used to divide the experiments in different wear classes. A classification is performed for two scenarios, a two- and three-class classification scenario.

4.1. Two class

Experiments with a w_V higher than $0,2\text{ mm}^3$ are labelled "Wear" and by implication lower values are labelled "No wear". The result of the classification can be seen in the confusion matrix in table 4. The table shows the mean value of the LOOCV for each case. It can be observed that the classifier is able to detect the occurrence of wear.

Table 4. Confusion Matrix for the two-classes scenario. The RFC is capable to detect the occurrence of wear.

		True Class	
		No wear	Wear
Predicted Class	No wear	91,7%	8,3%
	Wear	20,0%	80,0%

4.2. Three class

In order to test whether a more detailed classification is possible, a three-class scenario is carried out, although the number of experiments is low and their distribution among the different wear classes is unbalanced. In this scenario experiments w_V higher than $0,2\text{ mm}^3$ are labelled "Low wear", w_V higher than 1 mm^3 are labelled "High wear" and all other experiments are labelled "No wear". The distribution of wear-classes is shown in table 5. The distribution of the wear-classes is not uniform.

Table 5. Distribution of the wear-classes for the three-class scenario. The distribution of the wear-classes is not uniform.

Class	Bearing		
	0	1	2
No wear	4	2	7
Low wear	1	0	4
High wear	1	2	1

The confusion matrix of the classification is given in table 6. In this scenario, the classifier behaves in the same way when predicting "No wear", but performs slightly worse in terms of overall wear. The classifier performs poorly in distinguishing between "Low wear" and "High wear". However, the class "High wear" can clearly be distinguished from "No wear".

Table 6. Confusion Matrix for the three-classes scenario. The RFC performs poorly in distinguishing between "Low wear" and "High wear".

		True Class		
		No wear	Low wear	High wear
Predicted Class	No wear	91,7%	8,3%	0%
	Low wear	37,5%	50,0%	12,5%
	High wear	0%	33,3%	66,7%

4.3. Discussion

The results of the classification are promising and they support the assumption that a higher-resolution classification is possible. So far there are considerable misclassifications in the three-class scenario. Obvious reasons for this are the small number of experiments conducted and the distribution of wear among them.

A look at the feature importance for the three-class scenario in figure 8 shows that the number of bursts with high amplitude and the amplitude of the burst in general have the highest influence on the classification. The RMS of the AE signal and the envelope shortening can be seen to make a similarly large contribution. The characteristics in the frequency domain are given a rather low weight. Due to the small number of experiments carried out, a further feature-selection and feature-optimization did not seem to be informative.

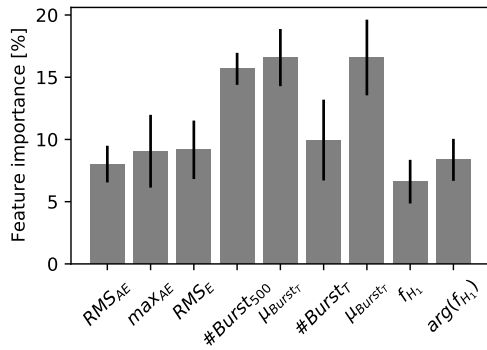


Figure 8. Feature importance (grey) for the three-class scenario with its standard deviation (black). The number of bursts with high amplitude and the amplitude of the burst in general have the highest influence on the classification.

5. CONCLUSION & OUTLOOK

The work presented shows that it is possible to use AE for the wear monitoring of a journal bearing by classifying wear during an experiment. The analysis of the AE signals confirmed the phenomena expected from earlier works regarding the connection between wear and AE in experimental setups. It can be shown that features generated from the measured AE signal and its envelope can be used to train a RFC to classify the severity of wear during operation even under non-constant operating conditions. So far it is not clear which aspect of the AE signal is most suitable for monitoring the wear.

Further improvements of this ongoing research will address several limitations of our work so far:

1. The detection and analysis of the bursts, the RMS and the envelope of the AE signal proves to be suitable for a classification of the wear rate. In order to better understand the significance of these actors, they will be analyzed in more detail. Therefore, they should be continuously monitored over the time of an experiment.
2. For a higher-resolution classification and with regard to regression, more experiments must be carried out. These experiments will be performed under constant operating conditions and each condition is applied to several bearings. In this way, the operating conditions can be decoupled from the wear, since each bearing can show a different wear behavior.
3. In preliminary work it proved difficult to determine the wear rate for an experiment in advance. Furthermore, in experiments with constant operating conditions, the wear is probably not distributed evenly over the course of an experiment. This assumption is supported by the observation that the RMS value of the AE signal usually flattens out towards the end of the experiment, see figure 7. In order to influence the wear rate, a controller is being developed which adapts the operating conditions in such

a way that in the ideal case the wear rate is kept constant.

4. With a view to implement a system for wear monitoring for journal bearings based on AE the biggest obstacle is the high sample rate necessary and the transmission of the data especially from hard to access sensor locations. The problem of the transmission of data is tackled by several works by transmitting the analog AE data wireless (Elasha et al., 2017; Mokhtari, Pelham, Nowoisky, Bote-Garcia, & Gühmann, 2020). By extracting good features or using only the envelope of the AE the sample rate and thus the amount of data for a system for online wear prediction can be scaled down drastically.

REFERENCES

- Albers, A., Burger, W., Scovino, R., & Dickerhof, M. (2006). Monitoring lubrication regimes in sliding bearings using acoustic emission analysis. *Practicing Oil Analysis*, 9(3), 8–12.
- Albers, A., & Dickerhof, M. (2010). Simultaneous monitoring of rolling-element and journal bearings using analysis of structure-born ultrasound acoustic emissions. In *Asme international mechanical engineering congress and exposition* (Vol. 44502, pp. 247–255).
- Boness, R., & McBride, S. (1991). Adhesive and abrasive wear studies using acoustic emission techniques. *Wear*, 149(1-2), 41–53.
- Breiman, L. (2001). Random forests. *Machine learning*, 45(1), 5–32.
- Chacon, J. L. F., Andicoberry, E. A., Kappatos, V., Asfis, G., Gan, T.-H., & Balachandran, W. (2014). Shaft angular misalignment detection using acoustic emission. *Applied acoustics*, 85, 12–22.
- Elasha, F., Greaves, M., Mba, D., & Fang, D. (2017). A comparative study of the effectiveness of vibration and acoustic emission in diagnosing a defective bearing in a planetary gearbox. *Applied Acoustics*, 115, 181–195.
- Hall, L. D., & Mba, D. (2004). Diagnosis of continuous rotor-stator rubbing in large scale turbine units using acoustic emissions. *Ultrasonics*, 41(9), 765–773.
- Hase, A., Mishina, H., & Wada, M. (2012). Correlation between features of acoustic emission signals and mechanical wear mechanisms. *Wear*, 292, 144–150.
- Hase, A., Mishina, H., & Wada, M. (2016). Fundamental study on early detection of seizure in journal bearing by using acoustic emission technique. *Wear*, 346, 132–139.
- Leahy, M., Mba, D., Cooper, P., Montgomery, A., & Owen, D. (2006). Experimental investigation into the capabilities of acoustic emission for the detection of shaft-to-seal rubbing in large power generation turbines: a case study. *Proceedings of the Institution of Mechanical Engineers, Part J: Journal of Engineering Tribology*, 220(7), 607–615.

- Li, Y., & Cheng, W. (2009). An online monitoring system of friction fault based on acoustic emission technology. In *2009 2nd international conference on power electronics and intelligent transportation system (peits)* (Vol. 1, pp. 329–332).
- Mokhtari, N., Knoblich, R., Nowoisky, S., Bote-Garcia, J.-L., & Gühmann, C. (2019). Differentiation of journal bearing friction states under varying oil viscosities based on acoustic emission signals. *2019 IEEE International Conference on Prognostics and Health Management (ICPHM)*, 1–7.
- Mokhtari, N., Pelham, J. G., Nowoisky, S., Bote-Garcia, J.-L., & Gühmann, C. (2020). Friction and Wear Monitoring Methods for Journal Bearings of Geared Turbofans Based on Acoustic Emission Signals and Machine Learning. *Lubricants*, 8(3), 29.

BIOGRAPHIES

José-Luis Bote-Garcia



M. Sc. José-Luis Bote-Garcia studied electrical engineering and computer science at the University of Applied Sciences of Aschaffenburg. During this time, he was in Mumbai via the DAAD (RISE Worldwide) for a research internship. Afterwards he completed a Master in Electrical Engineering at the Technical University of Berlin with a focus on automation technology. At this time he worked as a student assistant on the research project CargoCBM. He then started working as a research assistant at

the TU Berlin. Since the end of 2015 he has been employed at the Chair Electronic Measurement and Diagnostic Technology. He supervises lectures on the topics of measurement data processing and modeling of technical systems. His research focuses on the prediction of remaining useful lifetime on the example of journal bearings using machine learning.

Noushin Mokhtari



M. Sc. Noushin Mokhtari studied mechanical engineering at Leibniz University of Hanover and aerospace engineering at Technische Universität Braunschweig. Since 2015 she has been working as a research assistant at the Chair Electronic Measurement and Diagnostic Technology of Technische Universität Berlin. Her areas of expertise include the model and data based diagnosis and the lifetime prediction of hydrodynamic journal bearings, as well as signal processing, pattern recognition and classification of acoustic emission signals.

Clemens Gühmann



Prof. Dr.-Ing. Clemens Gühmann studied electrical engineering and has been head of the Chair Electronic Measurement and Diagnostic Technology since 2003 at the Technische Universität Berlin. His areas of expertise include the measurement technology and data processing as well as the diagnosis, modeling, simulation and automatic control of mechatronic systems.